Electrochemistry Communications 48 (2014) 81–85

Contents lists available at ScienceDirect

Electrochemistry Communications

journal homepage: www.elsevier.com/locate/elecom

Short communication

Stability of nanostructured iridium oxide electrocatalysts during oxygen evolution reaction in acidic environment

Serhiy Cherevko [a,1], Tobias Reier [b,1], Aleksandar R. Zeradjanin [a], Zarina Pawolek [b], Peter Strasser [b,*], Karl J.J. Mayrhofer [a,*]

[a] Department of Interface Chemistry and Surface Engineering, Max-Planck-Institut für Eisenforschung GmbH, Max-Planck-Straße 1, 40237 Düsseldorf, Germany
[b] Department of Chemistry, Technical University Berlin, Straße des 17. Juni 135, 10623 Berlin, Germany

ARTICLE INFO

Article history:
Received 29 July 2014
Received in revised form 27 August 2014
Accepted 27 August 2014
Available online 6 September 2014

Keywords:
Oxygen evolution
Energy conversion
Iridium oxide
IrO_2
Dissolution
Corrosion

ABSTRACT

The electrochemical stability of thermally prepared Ir oxide films is investigated using a scanning flow cell (SFC)–inductively coupled plasma mass-spectrometer (ICP-MS) setup under transient and stationary potential and/or current conditions. Time-resolved dissolution rates provide important insights into critical conditions for material breakdown and a fully quantitative in-situ assessment of the electrochemical stability during oxygen evolution reaction (OER) conditions. In particular, the results demonstrate that stability and OER activity of the IrO_x catalysts strongly depend on the chemical and structural nature of Ir oxide species and their synthesis conditions.

1. Introduction

Iridium oxide is a benchmark material for the (photo)-electrocatalytic oxygen evolution reaction (OER) in acidic media. Consequently, literature on the OER on Ir oxide is extensive [1–22]. Ir oxide species are usually divided into two categories, a highly defective amorphous and an anhydrous crystalline. It has been suggested repeatedly that the electrochemically prepared hydrated amorphous Ir oxide has a very high OER activity but suffers from severe corrosion [23–27]. Stabilization of hydrated amorphous Ir oxide can be achieved by heat treatment [28], therefore, the degree of hydration is supposed to be one important parameter for oxide stability [1]. Crystalline, anhydrated Ir oxide is believed to be more stable but less active for the OER and is a key component of industrially employed Dimensionally Stable Anodes (DSA) in electrolysis technology [29–31]. On the other hand, amorphous oxides are prone to corrosion during OER [20]. Interpretation of the experimental results obtained from such systems is however complicated, due to the complex mass transport and interactions between electrode components in a reactor. Recently, we presented a detailed study of how thermal treatment of IrO_x thin-film catalysts influences the OER kinetics [32–34]. What has remained unaddressed to date, however, concerns the correlation between geometric and electronic structure of the Ir oxide films and their electrochemical stability. This is the focus of the present study.

In the current work metallic iridium and thermally prepared iridium oxide thin-film model catalysts (on Ti substrates), fully characterized in terms of material properties and OER activity [32,33], are investigated using a scanning flow cell inductively coupled plasma mass spectrometry (SFC–ICP-MS) setup [35,36], and compared in terms of dissolution at conditions relevant to the OER.

2. Experimental

Thin iridium oxide films were prepared by spin coating of an Ir acetate precursor (thermally decomposable in air at 250 °C) on a Ti substrate and subsequent calcination in air according to [32,33]. Dissolution of metallic iridium was investigated on a polycrystalline Ir disk (MaTecK, Germany). All electrochemical and spectrometric measurements were performed using an SFC coupled with an ICP-MS (NexION 300X, Perkin Elmer) as described elsewhere [35,37,38]. The measurements were performed at room temperature applying 0.1 M perchloric acid (Merck Suprapur® 70% $HClO_4$ diluted using ultrapure water (PureLab Plus system, Elga, 18 MΩ, TOC < 3 ppb)) as electrolyte.

* Corresponding authors.
E-mail addresses: pstrasser@tu-berlin.de (P. Strasser), mayrhofer@mpie.de (K.J.J. Mayrhofer).
[1] These authors contributed equally to this work.

http://dx.doi.org/10.1016/j.elecom.2014.08.027

3. Results and discussion

Initial stability screening was performed by applying an electrode potential ramp starting at E = −0.05 V_{RHE} and ending at the potential where a current density j = 30 mA cm^{-2} was reached. Corresponding real-time dissolution profiles of Ir and Ti are shown in Fig. 1. Note that for clarity the scaling of the y-axis is different in each partial plot. As can be clearly seen from the graphs in Fig. 1, all samples except IrO_x@550 °C (here and below the numeric value represents the calcination temperature), start to dissolve already at low potentials. The amount of dissolved material increased when starting at a more negative potential. On the other hand no measurable amount of Ir was detected in the electrolyte when the ramp was started from open circuit potential (OCP ca. 0.9–1.0 V_{RHE}). Thus, we attribute this dissolution process to cathodic transient dissolution [38,39]. In terms of the amount of cathodically dissolved material, IrO_x@350 °C is the least stable oxide. Surprisingly, the highest dissolution peak was found on metallic Ir, which is most likely due to the reduction of the innate surface oxide formed in air. In this potential region no Ti dissolution was detected. The initial cathodic Ir dissolution decreased as the potential was swept anodically. Data in Fig. 1 evidences that at and above electrode potentials where the OER is thermodynamically possible, Ir dissolution initiates. IrO_x@550 °C exhibits the highest Ir dissolution and OER onset potential of E = 1.5 V_{RHE}. The dissolution rate measured at j = 30 mA cm^{-2} was used for a quantitative comparison of catalyst dissolution during the OER (see Table 1 below). IrO_x@550 °C is the most stable, while metallic Ir was found to be the least stable of all electrode materials investigated. The increased stability of the IrO_x@450 °C compared to the films calcined at 250 and 350 °C is likely correlated with the formation of a crystalline IrO_2 phase at 450 °C that was shown to exhibit a higher degree of lattice oxygen at the surface and consequently a lower degree of surface hydroxylation [32,33]. It seems plausible to conclude that crystalline order and lattice oxygen at the surface stabilize the Ir oxide against corrosion. At 550 °C calcination temperature, Ti diffuses into the Ir oxide layer and alters its chemical properties [32,33], which seem to result in further stabilization. Interestingly, the fully amorphous IrO_x@250 °C is by a factor of 4 more stable than the oxide film calcined at 350 °C, which is comprised of a mixture of the crystalline and the amorphous Ir oxide species. To explain the enhanced corrosion of the 350 °C film electrode, we therefore put forward the hypothesis that the coexistence of an amorphous and a crystalline phase is conducive to enhanced metal dissolution from the amorphous phase combined with metal ion transport, possibly at and along grain boundaries. In parallel to Ir, Ti dissolution was observed for all samples except for IrO_x@250 °C and metallic Ir, with a clear trend of increasing Ti dissolution with increase in the calcination temperature.

The operation of water electrolysers powered by renewable energy is expected to be intermittent, which may pose additional issues for catalyst stability [40,41]. To simulate fluctuating power inputs on the stability of the catalysts, consecutive square wave cycles with loads of j = 5 mA cm^{-2} over 3 s and idle breaks of j = 0 mA cm^{-2} over 3 s were applied. Corresponding dissolution profiles for Ir and Ti are shown in Fig. 2a and b, respectively, and the results are in line with those presented in Fig. 1. In particular, among all calcined Ir oxides IrO_x@350 °C was the least stable. Again, dissolution of Ti was observed on all calcined electrodes except IrO_x@250 °C. The amount of dissolved Ti for the three samples was similar. In the studied time interval dissolution of both metals did not reach a steady state value, although it is still possible to estimate dissolution tendency. At the end of the measurement, dissolution from the samples calcined at 450 °C and 550 °C was below the experimental detection limit of 0.5 pg cm^{-2} s^{-1} and 15 pg cm^{-2} s^{-1} (S/N = 3) for Ir and Ti, respectively. Initial Ir dissolution

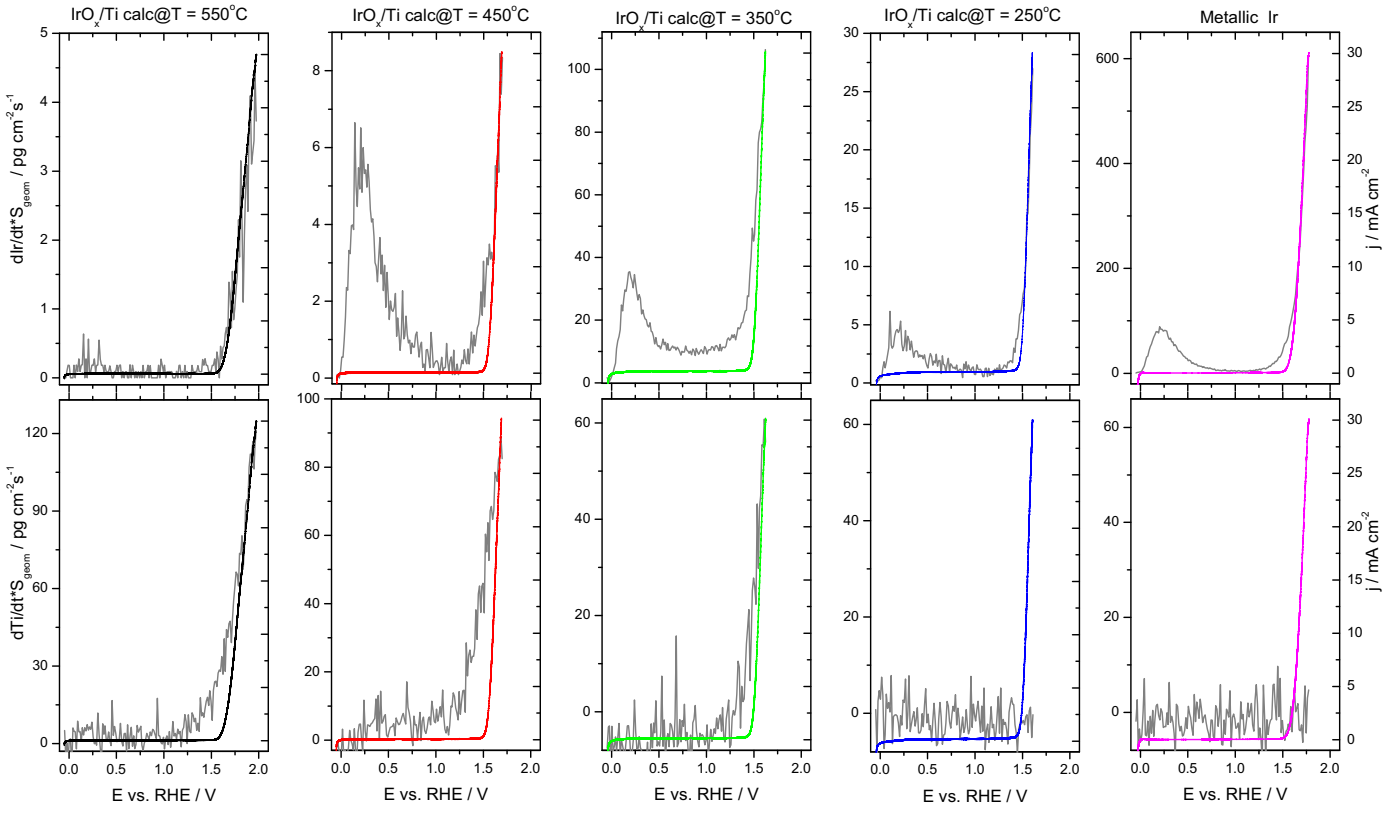

Fig. 1. Mass-spectrometric linear voltammograms (gray lines) and electrochemical linear voltammograms (colored lines) taken from four Ir oxide samples calcined at different temperatures and metallic Ir as indicated in the figure. Dissolution of Ir and Ti is presented in top and bottom row images, respectively. The potential was scanned from −0.05 V_{RHE} to a potential corresponding to current density of j = 30 mA cm^{-2} at which the scan was stopped and OCP was established. The scan rate was 10 mV s^{-1}.

Table 1
Summary of the electrochemical and mass-spectrometry data collected during the experiments.

#	T, °C	F, mC cm^{-2}	Dissolution during ramp (Fig. 1)			Fast square-wave pulses (Fig. 2)		j = 2 mA cm^{-2} (Fig. 3)	
			Ir (cathodic)	Ir (anodic)[a]	Ti (anodic)[a]	Ir	Ti	Ir	Ti
			ng cm^{-2}/ng mC						
1	–	–	3.2	60	–	90	–	13.3	–
2	250	12.4	0.24/0.02	1.68/0.14	–	2.0/0.16	–	1.06/0.09	–
3	350	7.5	1.58/0.21	7.3/0.97	5.2/0.69	9.2/1.23	8.2/1.09	4.1/0.55	1.3/0.17
4	450	2.1	0.24/0.11	0.47/0.22	9.0/4.29	0.66/0.31	10.4/4.95	0.29/0.14	2.9/1.38
5	550	0.65	–	0.25/0.38	9.9/15.23	0.27/0.42	8.2/12.61	0.16/0.25	2.8/4.31

[a] Integration was made over the dissolution curves presented in Fig. 1 including descending part which is not shown in the figure.

of IrO_x@250 °C was slightly higher, though, over longer time scales, it is clearly approaching the dissolution values of the samples annealed at higher temperatures. Consistent with the findings above, IrO_x@350 °C showed significant dissolution over the entire experiment. It should be noted that the dissolution rate of metallic Ir was at least one order of magnitude higher and is therefore not shown for clarity. The decrease in dissolution rate with time indicates irreversible surface passivation processes.

Quasi-steady-state operation was modeled applying two pulses with j = 1 mA cm^{-2} followed by j = 2 mA cm^{-2} over 600 s each as shown in Fig. 3a. In between, j = 0 mA cm^{-2} was applied for 180 s. Corresponding potential and Ir and Ti dissolution profiles are presented in Fig. 3b–c, respectively. In line with our previous work [33], electrodes calcined at T = 250 °C and T = 350 °C showed the highest activity (lower potential at a given current density). With increase in the calcination temperature, the activity drops. Nevertheless, even after calcination at T = 450 °C the activity was still higher than that of metallic Ir, which indicates that there is no simple trade-off between activity and stability. The transient nature of Ir and Ti dissolution shown in Fig. 2 is also reflected in Fig. 3. Immediately after the application of a current load of j = 1 mA cm^{-2} a sharp peak appeared on the mass-spectrograms. However, the dissolution rate of both metal oxides decreased very fast over the first 100 s, followed by a more gradual signal decay in the next 500 s. At OCP the dissolution rate decreased faster, though the signal still did not drop to the level of the blank. Some increase in Ir dissolution rate was observed when the next load of j = 2 mA cm^{-2} was applied, but not as pronounced as for the first step. It

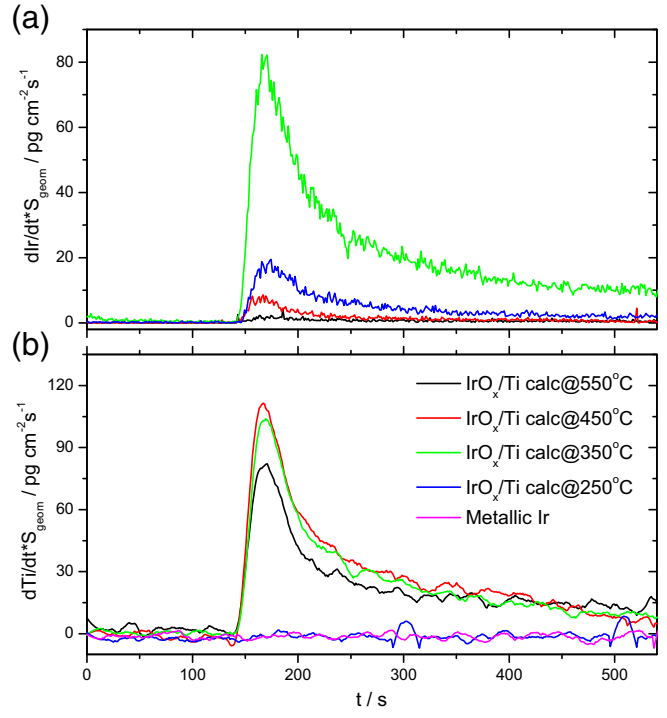

Fig. 2. Dissolution profiles of (a) Ir and (b) Ti during a square current pulse program as described in the main text.

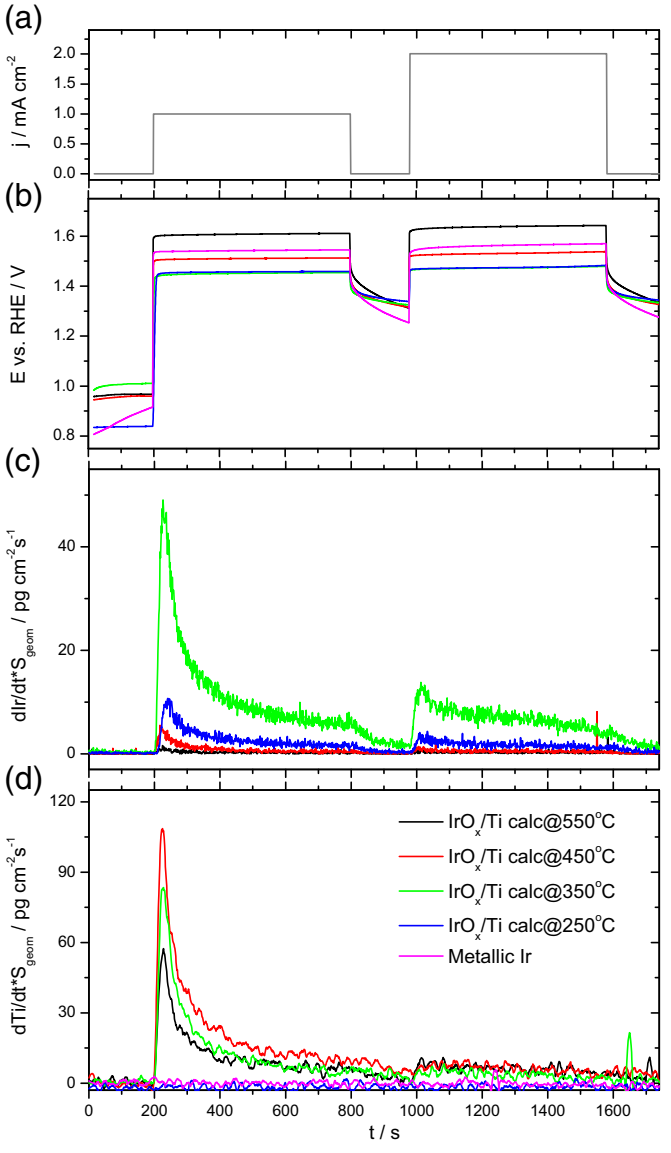

Fig. 3. Dissolution profiles of Ir and Ti during quasi-steady state load. Applied current program and potential response are shown in (a) and (b), respectively. Dissolution of Ir and Ti is presented in (c) and (d), respectively.

seems that the increase is due to certain reverse restructuring of the oxide taking place at OCP.

While the mechanism of the transient Ir corrosion appears similar for all Ir oxide films, the extent of Ir dissolution differs substantially between the samples. This is quantitatively summarized in Table 1. The amount of dissolved material is normalized to the geometric surface area of the electrodes. Previously, we have shown that IrO_x calcined at $T \geq 450$ °C consists of a porous layer with a pore size in the sub-10 nanometer range [33]. On the other hand, lower calcination temperatures result in visually pore-free compact layers. This brings some ambiguity in the quantification and comparison of dissolution data based only on geometric surface area. Thus, an alternative normalization to pseudo-capacitive charge (measured with 50 mV s^{-1} between 0.4 and 1.4 V) is also presented (highlighted in red). The pseudo-capacitance of Ir oxides decreases with calcination temperature as can be seen from the table. Much higher capacitance for pore-free samples may be attributed to the much higher number of redox active hydroxyl groups combined with enhanced proton diffusion in the hydrous Ir oxide [3]. The likely participation of water molecules inside the hydrous Ir or Ru oxide in the OER reaction creates a 3-dimensional reaction zone [25,38,39,42,43], and makes this type of normalization reasonable, although recent results show that in this reaction may be surface confined [44]. In terms of Ir and Ti dissolution normalized to the geometric surface area, the trends established in Figs. 1–3 are also reflected in Table 1. The picture changes, however, if normalization is made to capacitance, where IrO_x@250 °C exhibits the lowest dissolution.

4. Conclusions

The calcination temperature and the nature of the Ir oxide species have a strong impact on the Ir dissolution during conditions of the OER. The stability of thermally prepared Ir oxide films essentially increases with increasing calcination temperature. Importantly, the Ir oxide film prepared at an intermediate temperature of 350 °C breaks the trend and constitutes the least stable thermally prepared Ir oxide film. We hypothesize that this is due to the presence of a mixture of crystalline and amorphous Ir oxide phases. The Ir oxide film prepared at 250 °C is more stable than the IrO_x@350 °C, while their activity is basically the same. This observation suggests that there is not necessarily a tradeoff between activity and stability for OER catalysts. Ti dissolution, which occurs at and above a calcination temperature of 350 °C, is unproblematic, since only a small amount of Ti oxide formed during synthesis dissolves before the dissolution fades out.

Acknowledgments

This work was supported by the DFG Cluster of Excellence 'Unifying Concepts in Catalysis', the DFG grant STR 596/3-1 as part of the Priority Program 1613 "Regeneratively formed fuels by light driven water splitting" and BMBF (Kz: 033RC1101A).

References

[1] S. Trasatti, Transition metal oxides: versatile materials for electrocatalysis, in: J. Lipkowski, P.N. Ross (Eds.), The Electrochemistry of Novel Materials, VCH, 1994, (Ch. 5).
[2] S. Trasatti, Interfacial electrochemistry of conductive oxides for electrocatalysis, in: A. Wieckowski (Ed.), Interfacial Electrochemistry: Theory: Experiment, and Applications, Taylor & Francis, 1999, (Ch. 43).
[3] S. Trasatti, Physical electrochemistry of ceramic oxides, Electrochim. Acta 36 (1991) 225–241.
[4] Y.M. Kolotyrkin, V.V. Losev, A.N. Chemodanov, Relationship between corrosion processes and oxygen evolution on anodes made from noble metals and related metal oxide anodes, Mater. Chem. Phys. 19 (1988) 1–95.
[5] H. Tamura, C. Iwakura, Metal oxide anodes for oxygen evolution, Int. J. Hydrogen Energy 7 (1982) 857–865.
[6] S. Trasatti, Electrocatalysis: understanding the success of DSA®, Electrochim. Acta 45 (2000) 2377–2385.
[7] S. Trasatti, Electrocatalysis in the anodic evolution of oxygen and chlorine, Electrochim. Acta 29 (1984) 1503–1512.
[8] S. Trasatti, Electrocatalysis by oxides — attempt at a unifying approach, J. Electroanal. Chem. 111 (1980) 125–131.
[9] D.N. Buckley, L.D. Burke, The oxygen electrode. Part 6. — oxygen evolution and corrosion at iridium anodes, J. Chem. Soc. Faraday Trans. 1: Phys. Chem. Condens. Phases 72 (1976) 2431–2440.
[10] I. Katsounaros, S. Cherevko, A.R. Zeradjanin, K.J.J. Mayrhofer, Nanostructured electrocatalysts — oxygen electrochemistry as a cornerstone for sustainable energy conversion, Angew. Chem. Int. Ed. 53 (2014) 102–121.
[11] H. Dau, C. Limberg, T. Reier, M. Risch, S. Roggan, P. Strasser, The mechanism of water oxidation: from electrolysis via homogeneous to biological catalysis, ChemCatChem 2 (2010) 724–761.
[12] I.A. Lervik, M. Tsypkin, L.-E. Owe, S. Sunde, Electronic structure vs. electrocatalytic activity of iridium oxide, J. Electroanal. Chem. 645 (2010) 135–142.
[13] S. Fierro, T. Nagel, H. Baltruschat, C. Comninellis, Investigation of the oxygen evolution reaction on Ti/IrO2 electrodes using isotope labelling and on-line mass spectrometry, Electrochem. Commun. 9 (2007) 1969–1974.
[14] H. Elzanowska, J. Segal, V.I. Birss, Complications associated with kinetic studies of hydrous Ir oxide films, Electrochim. Acta 44 (1999) 4515–4524.
[15] P.G. Pickup, V.I. Birss, The kinetics of charging and discharging of iridium oxide films in aqueous and non-aqueous media, J. Electroanal. Chem. 240 (1988) 185–199.
[16] C.C.L. McCrory, S. Jung, J.C. Peters, T.F. Jaramillo, Benchmarking heterogeneous electrocatalysts for the oxygen evolution reaction, J. Am. Chem. Soc. 135 (2013) 16977–16987.
[17] H.N. Nong, L. Gan, E. Willinger, D. Teschner, P. Strasser, IrOx core-shell nanocatalysts for cost- and energy-efficient electrochemical water splitting, Chem. Sci. 5 (2014) 2955–2963.
[18] E. Ortel, T. Reier, P. Strasser, R. Kraehnert, Mesoporous IrO2 films templated by PEO-PB-PEO block-copolymers: self-assembly, crystallization behavior, and electrocatalytic performance, Chem. Mater. 23 (2011) 3201–3209.
[19] V.V. Gorodetskii, V.A. Neburchilov, Titanium anodes with active coatings based on iridium oxides: the corrosion resistance and electrochemical behavior of anodes coated by mixed iridium, ruthenium, and titanium oxides, Russ. J. Electrochem. 41 (2005) 971–978.
[20] V.V. Gorodetskii, V.A. Neburchilov, Tantalum oxide effect on the surface structure and morphology of the IrO2 and IrO2 + RuO2 + TiO2 coatings and on the corrosion and electrochemical properties of anodes prepared from these, Russ. J. Electrochem. 43 (2007) 223–228.
[21] R. Kotz, S. Stucki, Stabilization of RuO2 by IrO2 for anodic oxygen evolution in acid media, Electrochim. Acta 31 (1986) 1311–1316.
[22] K.-I. Fukuda, C. Iwakura, H. Tamura, Effect of heat treatment of ti substrate on service life of ti-supported IrO2 electrode in mixed aqueous solutions of H2SO4, (NH4)2SO4 and NH4F, Electrochim. Acta 25 (1980) 1523–1525.
[23] G. Beni, L.M. Schiavone, J.L. Shay, W.C. Dautremont-Smith, B.S. Schneider, Electrocatalytic oxygen evolution on reactively sputtered electrochromic iridium oxide films, Nature 282 (1979) 281–283.
[24] S. Gottesfeld, S. Srinivasan, Electrochemical and optical studies of thick oxide layers on iridium and their electrocatalytic activities for the oxygen evolution reaction, J. Electroanal. Chem. 86 (1978) 89–104.
[25] E.J. Frazer, R. Woods, The oxygen evolution reaction on cycled iridium electrodes, J. Electroanal. Chem. 102 (1979) 127–130.
[26] D.N. Buckley, L.D. Burke, The oxygen electrode. Part 5. — enhancement of charge capacity of an iridium surface in the anodic region, J. Chem. Soc. Faraday Trans. 1: Phys. Chem. Condens. Phases 71 (1975) 1447–1459.
[27] D. Burke, M.E.G. Lyons, Electrochemistry of hydrous oxide films, in: J.O.M. Bockris, B.E. Conway, R.E. White (Eds.), Modern Aspects of Electrochemistry, 28, Plenum Press, 1996.
[28] M. Vuković, Oxygen evolution reaction on thermally treated iridium oxide films, J. Appl. Electrochem. 17 (1987) 737–745.
[29] J. Krysa, J. Maixner, R. Mraz, I. Rousar, Effect of coating thickness on the properties of IrO_2–Ta_2O_5 anodes, J. Appl. Electrochem. 28 (1998) 369–372.
[30] J.M. Hu, H.M. Meng, J.Q. Zhang, C.N. Cao, Degradation mechanism of long service life Ti/IrO_2–Ta_2O_5 oxide anodes in sulphuric acid, Corros. Sci. 44 (2002) 1655–1668.
[31] L.K. Xu, J.D. Scantlebury, Microstructure and electrochemical properties of IrO_2–Ta_2O_5-coated titanium anodes, J. Electrochem. Soc. 150 (2003) B254–B261.
[32] T. Reier, I. Weidinger, P. Hildebrandt, R. Kraehnert, P. Strasser, Electrocatalytic oxygen evolution reaction on iridium oxide model film catalysts: influence of oxide type and catalyst substrate interactions, ECS Trans. 58 (2013) 39–51.
[33] T. Reier, D. Teschner, T. Lunkenbein, A. Bergmann, S. Selve, R. Kraehnert, R. Schlögl, P. Strasser, Electrocatalytic oxygen evolution on iridium oxide: uncovering catalyst–substrate interactions and active iridium oxide species, J. Electrochem. Soc. 161 (2014) F876–F882.
[34] B. Johnson, F. Girgsdies, G. Weinberg, D. Rosenthal, A. Knop-Gericke, R. Schlögl, T. Reier, P. Strasser, Suitability of simplified (Ir, Ti)Ox films for characterization during electrocatalytic oxygen evolution reaction, J. Phys. Chem. C 117 (2013) 25443–25450.
[35] S.O. Klemm, A.A. Topalov, C.A. Laska, K.J.J. Mayrhofer, Coupling of a high throughput microelectrochemical cell with online multielemental trace analysis by ICP-MS, Electrochem. Commun. 13 (2011) 1533–1535.
[36] S. Cherevko, A.A. Topalov, I. Katsounaros, K.J.J. Mayrhofer, Electrochemical dissolution of gold in acidic medium, Electrochem. Commun. 28 (2013) 44–46.
[37] S. Cherevko, A.A. Topalov, A.R. Zeradjanin, I. Katsounaros, K.J.J. Mayrhofer, Gold dissolution: towards understanding of noble metal corrosion, RSC Adv. 3 (2013) 16516–16527.

[38] S. Cherevko, A.R. Zeradjanin, A.A. Topalov, N. Kulyk, I. Katsounaros, K.J.J. Mayrhofer, Dissolution of noble metals during oxygen evolution in acidic media, ChemCatChem 6 (2014) 2219–2223.
[39] B.E. Conway, J. Mozota, Surface and bulk processes at oxidized iridium electrodes — II. Conductivity-switched behaviour of thick oxide films, Electrochim. Acta 28 (1983) 9–16.
[40] S. Trasatti, Electrochemistry and environment: the role of electrocatalysis, Int. J. Hydrogen Energy 20 (1995) 835–844.
[41] J. Divisek, J. Mergel, H. Schmitz, Advanced water electrolysis and catalyst stability under discontinuous operation, Int. J. Hydrogen Energy 15 (1990) 105–114.
[42] A.R. Hillman, M.A. Skopek, S.J. Gurman, X-Ray spectroscopy of electrochemically deposited iridium oxide films: detection of multiple sites through structural disorder, Phys. Chem. Chem. Phys. 13 (2011) 5252–5263.
[43] K. Macounova, M. Makarova, P. Krtil, Oxygen evolution on nanocrystalline RuO2 and Ru0.9Ni0.1O2 − δ electrodes — DEMS approach to reaction mechanism determination, Electrochem. Commun. 11 (2009) 1865–1868.
[44] H.G. Sanchez Casalongue, M.L. Ng, S. Kaya, D. Friebel, H. Ogasawara, A. Nilsson, In situ observation of surface species on iridium oxide nanoparticles during the oxygen evolution reaction, Angew. Chem. Int. Ed. 53 (2014) 7169–7172.